Effect of shallow cumulus convection on the eastern Pacific climate in a coupled model

Simon P. de Szoeke,[1] Yuqing Wang,[1] Shang-Ping Xie,[1] and Toru Miyama[2]

Received 26 April 2006; revised 28 June 2006; accepted 25 July 2006; published 12 September 2006.

[1] Shallow cumulus convection evaporates stratocumulus clouds in the atmospheric boundary layer. The effect of shallow convection on the large-scale climate of the eastern tropical Pacific is investigated with a coupled ocean-atmosphere model by disabling the shallow convection parameterization (noSC). Without shallow convection, the stratiform cloud fraction increases and surface solar radiation decreases. The sea surface temperature (SST) cools on average by 2°C. The cooling in noSC is larger under the low cloud deck south of the equator than north of the equator, resulting in an increase in the climatic meridional asymmetry. In the control run an ITCZ forms south of the equator in March-April. In noSC the SST is at most 24°C south of the equator and an ITCZ does not form. The perennial northern-hemisphere ITCZ in noSC is accompanied by year-round southerlies of at least $\sim$3 m s^{-1} on the equator, considerably reducing the seasonal cycle of equatorial SST. **Citation:** de Szoeke, S. P., Y. Wang, S.-P. Xie, and T. Miyama (2006), Effect of shallow cumulus convection on the eastern Pacific climate in a coupled model, *Geophys. Res. Lett.*, *33*, L17713, doi:10.1029/2006GL026715.

1. Introduction

[2] Simulation of the eastern Pacific climate and its variability, including El Nino/Southern Oscillation (ENSO), is improving in coupled global climate models (CGCMs) [*Wang et al.*, 2005; *Wittenberg et al.*, 2006; *Large and Danabasoglu*, 2006], but CGCMs suffer biases, including a cold bias at the equator, a warm bias off the coast of South America, a double-ITCZ straddling the equator, and biases in the seasonal cycle. These model biases can be exacerbated or compensated by the positive feedback between low clouds and cold sea surface temperature (SST) [e.g., *Mechoso et al.*, 1995]. The parameterization of shallow cumulus convection is a source of uncertainty in climate models, which has a significant effect on the simulated low cloud.

[3] Shallow cumulus convection plays an important role in determining the fraction of low clouds in the tropics and subtropics. Shallow cumulus clouds have little horizontal extent but occur frequently in regions of large surface heat fluxes, particularly in the trade-wind regions over the tropical and subtropical oceans. In these regions, extensive stratus and stratocumulus cloud decks cool the ocean by reflecting sunlight back to space [*Hartmann et al.*, 1992]. Shallow cumulus updrafts penetrate the inversion that caps the planetary boundary layer (PBL). The updrafts entrain warm dry air into the PBL and weaken the inversion. By deepening the PBL and evaporating stratus and stratocumulus clouds, shallow cumulus clouds bring about a transition from stratocumulus to trade cumulus cloud regimes [*Albrecht et al.*, 1995], causing cloudiness to decrease.

[4] While eddy-resolving models [*Wyant et al.*, 1997] and large eddy simulations [*de Szoeke and Bretherton*, 2004] have simulated the interplay of stratocumulus and shallow cumulus clouds by resolving cloud-scale circulations, shallow cumulus convection has to be parameterized in large-scale models. In this regard, mass-flux schemes [e.g., *Tiedke*, 1989] are popular for parameterizing shallow cumulus convection in numerical weather prediction and climate models. The effect of disabling the shallow convection parameterizations in these atmospheric models is to unrealistically increase the stratiform cloud amount, to reduce the surface evaporation, and to reduce the free-tropospheric humidity [*McCaa and Bretherton*, 2004; *Wang et al.*, 2004b; *von Salzen et al.*, 2005].

[5] Previous atmospheric modeling studies with prescribed SST ignored the positive feedback between low clouds and SST. This study investigates this feedback by performing experiments with a coupled ocean-atmosphere model of the eastern Pacific. We show that shallow cumulus convection affects not only low clouds, but also the large-scale structures and the seasonal cycle of the eastern Pacific climate.

[6] The next section briefly introduces the model, the shallow cumulus convection scheme, and the experimental design. Section 3 discusses the effect of shallow cumulus convection on the seasonal mean simulation of the clouds and on the lower-tropospheric vertical structure. The effect of the shallow convection on the meridional asymmetry and the seasonal cycle of the eastern tropical Pacific climate is discussed in section 4. A summary is presented in section 5.

2. Model Description

[7] The model used in this study is the International Pacific Research Center (IPRC) Regional Ocean Atmosphere Model (IROAM) (S.-P. Xie et al., A regional ocean-atmosphere model for eastern Pacific climate: Towards reducing tropical biases, submitted to *Journal of Climate*, 2006, hereinafter referred to as Xie et al., submitted manuscript, 2006): IROAM is configured as a tropical Pacific Ocean general circulation model (MOM2) [*Pacanowski*, 1995] coupled to a regional atmospheric model of the eastern Pacific. The atmospheric model is the IPRC Regional Atmospheric Model, which has been

[1]International Pacific Research Center, University of Hawaii, Honolulu, Hawaii, USA.
[2]Frontier Research Center for Global Change, Japan Agency for Marine-Earth Science and Technology, Yokohama, Japan.

0094-8276/06/2006GL026715$05.00

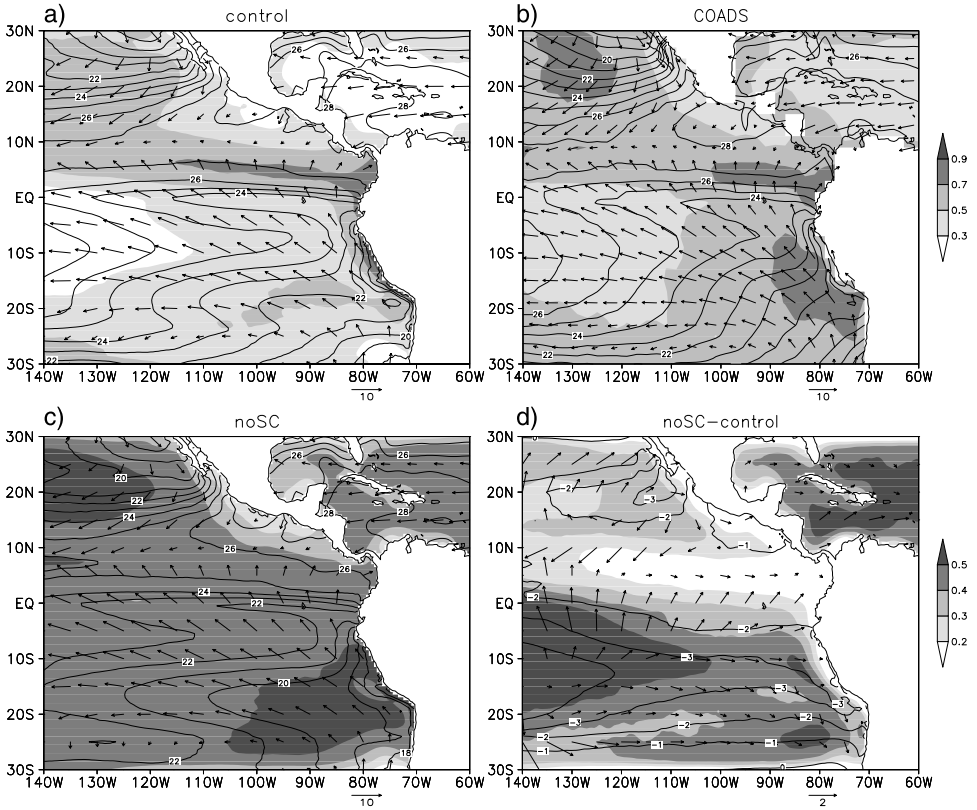

Figure 1. The annual mean cloud fraction (shaded), SST (°C contours), and surface wind vectors m s^{-1} for (a) the control simulation, (b) COADS observations, and (c) noSC. The upper color scale applies to panels (a-c). (d) Difference between noSC and the control run (noSC—control).

used previously to simulate the boreal summer climate over the eastern Pacific with prescribed SST [*Wang et al.*, 2004a]. The latitudinal boundaries for the ocean and atmosphere are at 35°N and 35°S, and the regional atmosphere extends from 150° to 30°W. The lateral boundary conditions for the regional atmospheric model and the surface conditions for the ocean model west of 150°W are prescribed by the National Center for Atmospheric Research/National Center for Environmental Prediction (NCEP) reanalysis [*Kistler et al.*, 2001].

[8] The IROAM atmosphere uses a mass flux convection parameterization [*Tiedke*, 1989] for deep, mid-level, and shallow cumulus convection, with a convective available potential energy (CAPE) closure [*Nordeng*, 1994] for deep convection. Deep and shallow convection are triggered under conditionally unstable conditions by the total column moisture source, including resolved-scale convergence and surface evaporation. Compared to deep cumulus convection, shallow cumulus are assumed to be nonprecipitating, and to have smaller updraft plumes that mix more effectively with the environment. The convection scheme supports only one category of convection in each grid per time step. Deep convection is assumed to occur if the column moisture convergence is greater than 10% of the local surface evaporation, and the diagnosed cloud thickness is 200 hPa or thicker. Otherwise shallow convection is assumed. Mid-level convection is triggered by moisture convergence well above the boundary layer, typically by large-scale ascent.

[9] Here we present a simulation with standard settings (hereafter *control*) as by Xie et al. (submitted manuscript, 2006) and a sensitivity experiment in which the shallow convection is forbidden (*noSC*). The coupled simulations start when the atmospheric model is initialized with NCEP initial conditions in 1996, after the ocean model has spun up from *Levitus* [1982] climatology for five years. The first two years of the coupled integration are considered to be model spin up, and the six-year average from 1998–2003 is considered to be the climatology of the model.

3. Mean Clouds and SST

[10] The spatial pattern of the annual mean SST in the IROAM control simulation agrees well with COADS ship observations (Figures 1a and 1b). The IROAM control simulation produces a spatial pattern of cloud fraction similar to COADS, but underestimates cloud fraction by about 0.1 relative to COADS. The largest underestimate is in the cold-season stratus cloud off the coast of California and the coasts of Peru and northern Chile in the second half of the year. The highest cloud fraction in the control run is found in a zonal belt of transitional cloud between the equator and the ITCZ.

[11] The annual average cloud fraction, SST, and surface wind vectors from noSC are shown in Figure 1c. The spatial distribution of the clouds, SST, and winds are similar to the control simulation in Figure 1a, however in noSC the cloud fraction is increased by 0.1–0.6. The increase of clouds in noSC is consistent with previous modeling studies [*McCaa*

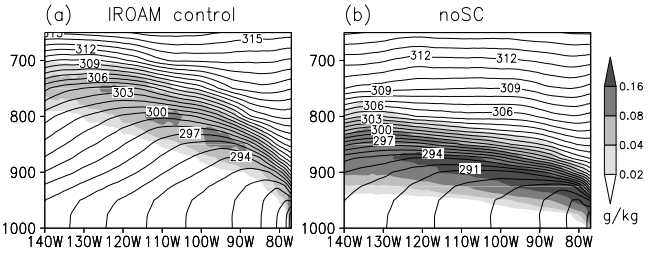

Figure 2. IROAM September vertical (pressure, hPa)-longitude sections along 15°S of potential temperature (contoured, K) and cloud liquid water mixing ratio (shaded, g kg^{-1}) for (a) the control run and (b) noSC.

and Bretherton, 2004; *Wang et al.*, 2004b; *von Salzen et al.*, 2005].

[12] Figure 1d shows the difference between noSC and the control simulation. Because of the increase in cloudiness, the SST is decreased on the whole by about 2°C. Around 15°S the SST in noSC is reduced by 3–4°C, with the largest reduction in the trade-wind region west of 120°W, downstream of the observed southern-hemisphere tropical stratocumulus deck. This region is characterized by cold advection and surface evaporation, where the shallow convection is quite active in venting the PBL in the control simulation. Without shallow cumulus convection, the stratus clouds persist and reduce the SST around 10°S on the southern edge of the southern-hemisphere SST maximum. Removing shallow convection does not affect the cloud fraction as much in regions where stratus clouds are relatively solid and shallow convection is less active, such as over cold SST or below a strong capping inversion.

[13] The cloud fraction in noSC is increased by only 0.2 in the cold-advection region between the equator and 10°N. In this region, the SST is high with a large meridional gradient and the wind speed is strong, causing large surface heat fluxes that are favorable for shallow convection. The clouds found here are mixed shallow cumulus and stratocumulus. The removal of shallow cumulus clouds in noSC is compensated by stratocumulus clouds generated by the vertical mixing of the PBL turbulence scheme.

[14] Shallow convection modifies the vertical structure of the PBL and lower troposphere. Figure 2 shows the vertical structure of the potential temperature and cloud water mixing ratio in September along 15°S for the control run and noSC. A deck of stratiform clouds is seen at the top of the PBL beneath a stable capping inversion. At the South American coast near 80°W the cloud deck is very low, reaching 1000 hPa in both simulations. The clouds rise as the SST warms to the west. In the control simulation (Figure 2a) the cloud layer rises steeply to the west. The highest cloud top reaches 700 hPa around 130°W. The clouds above 900 hPa west of 95°W are atop a moist-adiabatic layer, which decouples the surface mixed layer and the cloud layer. In noSC there is no moist-adiabatic layer and the stratus cloud base is always below 900 hPa (Figure 2b). The clouds in noSC are coupled to the top of the surface mixed layer through turbulent mixing. The cloud liquid water mixing ratio is about twice as large for noSC as compared to the control run.

[15] The change in the SST between noSC and the control run is not simply forced by the change in the clouds, but also involves the feedback between the SST and clouds. The decrease of SST due to increased cloud cover in noSC reduces the boundary layer temperature, which promotes condensation and increases the stability of the capping inversion (Figure 2). The stronger inversion discourages entrainment of dry air into the PBL, thereby limiting the evaporation of cloud water and increasing low clouds [*Klein and Hartmann*, 1993]. The reduction of the SST enhances the high pressure below the stratus decks. Subsidence above the high pressure further caps the PBL inversion. Enhanced divergence of the surface winds are seen from the cold anomaly at 10–20°S west of 120°W (Figure 1d). These changes contribute to the large increase in cloud fraction in this region.

4. Meridional Asymmetry and the Seasonal Cycle

[16] The increase of cloudiness and the decrease of SST in noSC are larger south of the equator where the PBL is capped by stratocumulus clouds. The increase in cloud fraction is less than 0.3 along 10°N as opposed to greater than 0.4 along 10°S. As a result, the meridional asymmetry of the eastern Pacific climate strengthens in noSC, with the ITCZ staying north of the equator year-round (Figure 3b). The annual-mean cross-equatorial southerlies increase by 1–2 m s^{-1} (Figure 1d).

[17] This enhanced meridional asymmetry of SST affects the seasonal cycle in several ways. Figure 3a shows the seasonal cycle of precipitation (shaded), SST (contoured), and wind vectors averaged between 90 and 110°W for the control run. In March-April, the meridional asymmetry of the SST about the equator becomes weak. The SST warms

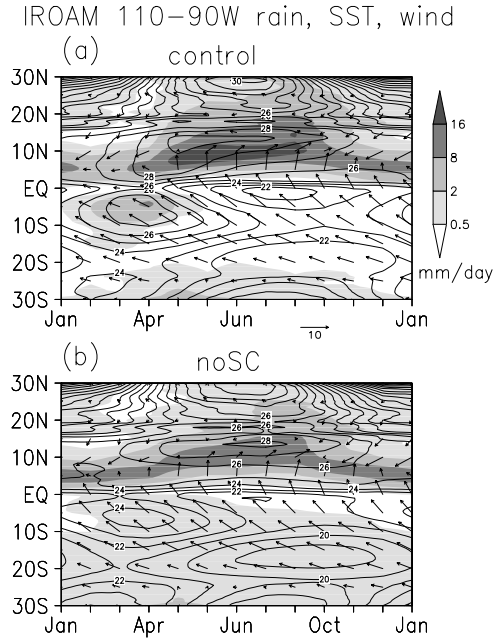

Figure 3. Seasonal cycle of rain (mm day^{-1}, shaded), SST (°C, contoured), and surface wind vectors from the IROAM (a) control run and (b) noSC. The legend vector represents a wind speed of 10 m s^{-1}.

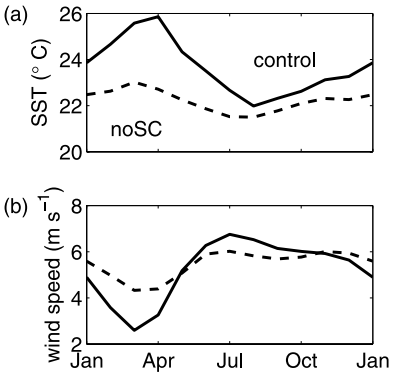

Figure 4. Seasonal cycle of equatorial (a) SST and (b) vector wind speed averaged from 90–120°W for the control simulation (solid) and noSC (dashed).

above 27°C south of the equator between 2–9°S. For this brief season, deep convection forms in the southern hemisphere and the ITCZ straddles the equator. The southeasterly wind usually found on the equator weakens between the two ITCZs in March-April and the equatorial SST warms in the absence of strong upwelling and vertical mixing in the upper ocean [*Mitchell and Wallace*, 1992; *Xie*, 1994]. In noSC, the anomalous cooling due to the additional stratiform clouds reduces the SST in the southern hemisphere, enhancing the meridional asymmetry of the SST. Even in March-April the southeast tropical Pacific SST is at most 24°C, too cold for the ITCZ to form in the southern hemisphere. The ITCZ stays in the northern hemisphere (Figure 3b), and its precipitation amount has a weaker seasonal cycle than in the control run. Thus year-round southerlies blow across the equator, and the equatorial SST stays cold, barely reaching 23°C in March. Drizzle in the southern stratocumulus deck increases in noSC. Drizzle drys the PBL, offsetting the lack of entrainment drying from shallow convection.

[18] The seasonal cycle of SST at the equator (averaged between 120°W and 90°W) for the control simulation and noSC is shown in Figure 4a. The warm season SST in March and April is reduced by 2.5°C in noSC. The colder equatorial temperature in March is explained by the 2 m s^{-1} stronger wind in noSC, which continues to drive upwelling and stirring of cold thermocline water into the surface mixed layer at a considerably higher rate than in the control simulation (Figure 4b). The increased clouds in noSC also reduce the solar heating of the ocean in March.

5. Summary

[19] A control simulation and a simulation with no shallow convection (noSC) by the IPRC coupled Regional Ocean Atmosphere Model (IROAM) demonstrate the effect of shallow cumulus convection in maintaining a realistic climatology of the eastern tropical Pacific. The southern hemisphere in the eastern Pacific is climatologically cooler than the northern hemisphere. As observed, the control run exhibits a brief warm season in March-April when the SST in the southern hemisphere warms enough for an ITCZ to form on each side of the equator. In the warm season the meridional temperature gradient and winds become weak across the equator, reducing upwelling and vertical mixing on the equator and allowing the equatorial SST to warm.

[20] In noSC the SST cools 1–4°C in response to the reduction of insolation by the clouds. The increase in clouds due to the removal of shallow convection preferentially cools the southern tropical stratocumulus region, increasing the meridional temperature asymmetry. Many coupled models suffer a double ITCZ syndrome, with the ITCZ lingering too long south of the equator [*Mechoso et al.*, 1995]. The simulation entirely without shallow convection achieves an opposite extreme with a year-round single northern ITCZ; the maximum temperature south of the equator is 24°C. Southeasterly winds persist on the equator year-round, weakening the seasonal cycle of equatorial upwelling and keeping the equatorial SST cold.

[21] Shallow convection vents moisture out of the PBL and entrains dry air in, evaporating clouds and deepening the PBL. The cloud fraction is increased by 0.1–0.6 in the simulation with no shallow convection. In noSC the cloud layer is lower and coupled to the turbulent surface mixed layer. Drizzle and light rain are enhanced in the southern stratiform cloud region in noSC. Shallow convection and drizzle both dry the PBL and reduce radiatively important low clouds, but the evaporation of drizzle stabilizes the upper PBL, while shallow convection destabilizes the lower troposphere by evaporation of cloud water above the PBL.

[22] Previous studies on the effect of shallow convection in atmosphere-only models have focused on the cold season, when the southern stratocumulus clouds are maximal, and not on the seasonal cycle. Our coupled simulations show that departures of SST in noSC peak in March-April. The meridional circulations in March–April are not changed as dramatically in models with prescribed SST.

[23] **Acknowledgments.** This work has been funded by the Japanese Ministry of Education, Culture, Sports, Science and Technology (MEXT) as category 7 of the RR2002 Project, by JAMSTEC, and by the United States National Oceanic and Atmospheric Administration (NOAA). The numerical calculation was carried out at the Earth Simulator Center. We also acknowledge Sharon DeCarlo, Yingshuo Shen, and Kazutoshi Horiuchi, who have diligently maintained our access to the IROAM data. This is IPRC contribution number 390 and SOEST contribution number 6795.

References

Albrecht, B. A., C. S. Bretherton, D. Johnson, W. H. Schubert, and A. S. Frisch (1995), The Atlantic stratocumulus transition experiment—ASTEX, *Bull. Am. Meteorol. Soc.*, *76*(6), 889–904.

de Szoeke, S. P., and C. S. Bretherton (2004), Quasi-Lagrangian large eddy simulations of cross-equatorial flow in the east Pacific atmospheric boundary layer, *J. Atmos. Sci.*, *61*(15), 1837–1858.

Hartmann, D. L., M. Ockert-Bell, and M. L. Michelsen (1992), The effect of cloud type on Earth's energy balance: Global analysis, *J. Clim.*, *5*(11), 1281–1304.

Kistler, R., et al. (2001), The NCEP/NCAR 50-year reanalysis: Monthly means CD-ROM and documentation, *Bull. Am. Meteorol. Soc.*, *82*(2), 247–267.

Klein, S. A., and D. L. Hartmann (1993), The seasonal cycle of low stratiform clouds, *J. Clim.*, *6*, 1588–1606.

Large, W. G., and G. Danabasoglu (2006), Attribution and impacts of upper ocean biases in CCSM3, *J. Clim.*, *19*, 2325–2346.

Levitus, S. E. (1982), *Climatological Atlas of the World Ocean*, *Prof. Pap. 13*, 173 pp., NOAA, Silver Spring, Md.

McCaa, J. R., and C. S. Bretherton (2004), A new parameterization for shallow cumulus convection and its application to marine subtropical cloud-topped boundary layers. Part II: Regional simulations of marine boundary layer clouds, *Mon. Weather Rev.*, *132*, 883–896.

Mechoso, C. R., et al. (1995), The seasonal cycle over the tropical Pacific in coupled ocean-atmosphere general circulation models, *Mon. Weather Rev.*, *123*, 2825–2838.

Mitchell, T. P., and J. M. Wallace (1992), The annual cycle in equatorial convection and sea surface temperature, *J. Clim.*, *5*, 1140–1156.

Nordeng, T. E. (1994), Extended versions of the convective parameterization scheme at ECMWF and their impact on the mean and transient activity of the model in the tropics, *Tech. Rep. 206*, Eur. Cent. for Medium-Range Weather Forecasts, Reading, U. K.

Pacanowski, R. C. (1995), MOM 2 documentation, user's guide and reference manual, version 1.0, Ocean Group Tech. Rep. 3, Geophys. Fluid Dyn. Lab., Princeton, N. J.

Tiedke, M. (1989), A comprehensive mass flux scheme for cumulus parameterization in large-scale models, *Mon. Weather Rev.*, *117*, 1779–1800.

von Salzen, K., N. A. McFarlane, and M. Lazare (2005), The role of shallow convection in the water and energy cycles of the atmosphere, *Clim. Dyn.*, *25*, 671–688.

Wang, W., S. Saha, H.-L. Pan, S. Nadiga, and G. White (2005), Simulation of ENSO in the new NCEP Coupled Forecast System model (CFS03), *Mon. Weather Rev.*, *133*, 1574–1593.

Wang, Y., S.-P. Xie, H. Xu, and B. Wang (2004a), Regional model simulations of marine boundary layer clouds over the southeast Pacific off South America. Part I: Control experiment, *Mon. Weather Rev.*, *132*(1), 274–296.

Wang, Y., H. Xu, and S.-P. Xie (2004b), Regional model simulations of marine boundary layer clouds over the southeast Pacific off South America. Part II: Sensitivity experiments, *Mon. Weather Rev.*, *132*(1), 2650–2668.

Wittenberg, A. T., A. Rosati, N.-C. Lau, and J. J. Ploshay (2006), GFDL's CM2 global coupled climate models. Part III: Tropical Pacific climate and ENSO, *J. Clim.*, *19*, 698–722.

Wyant, M. C., C. S. Bretherton, H. A. Rand, and D. E. Stevens (1997), Numerical simulations and a conceptual model for the stratocumulus to trade cumulus transition, *J. Atmos. Sci.*, *54*(1), 168–192.

Xie, S. P. (1994), On the genesis of the equatorial annual cycle, *J. Clim.*, *7*, 2008–2013.

S. P. de Szoeke, Y. Wang, and S.-P. Xie, International Pacific Research Center, University of Hawaii, 2525 Correa Road, Honolulu, HI 96822, USA. (deszoeke@hawaii.edu)

T. Miyama, Frontier Research Center for Global Change, JAMSTEC, 3173-25 Showamachi, Kanazawa-ku, Yokohama, Japan.